

# Target Residues Formed in the Deuteron-Induced Reaction of Gold at Incident Energy 2.2 AGeV

A. R. Balabekyan<sup>a</sup>, N. A. Demekhina<sup>b</sup>, G. S. Karapetyan<sup>c</sup>, D. R. Drnoyan<sup>d</sup>, V.I.Zhemenik<sup>d</sup>, J.Adam<sup>d</sup>, L.Zavoroka<sup>d</sup>, A.A.Solnyshkin<sup>d</sup>, V.M.Tsoupko-Sitnikov<sup>d</sup>, J.Khushvaktov<sup>d</sup>, L. Karayan<sup>a</sup>, A. Deppman<sup>c</sup>, V. Guimarães<sup>c</sup>

*a) Yerevan State University*

*A. Manoogian, 1, 025, Yerevan, Armenia*

*b) Yerevan Physics Institute,*

*Alikhanyan Brothers 2, Yerevan 0036, Armenia*

*Joint Institute for Nuclear Research (JINR),*

*Flerov Laboratory of Nuclear Reactions (LNR),*

*Joliot-Curie 6, Dubna 141980, Moscow region Russia*

*c) Instituto de Fisica, Universidade de São Paulo*

*Rua do Matao, Travessa R 187,*

*05508-900 São Paulo, SP, Brazil*

*d) Joint Institute for Nuclear Research (JINR),*

*Laboratory of Nuclear Problems (LNP),*

*Joliot-Curie 6, Dubna 141980, Moscow region Russia*

The cross sections of 110 radioactive nuclide with mass numbers  $22 \leq A \leq 198$  amu from the interaction of 2.2 GeV/nucleon deuterons from the Nuclotron of the Laboratory of High Energies (LHE), Joint Institute for Nuclear Research (JINR) at Dubna with a <sup>197</sup>Au target are investigated using induced activity method. The results including charge and mass distributions are parameterized in terms of 3-parameter equation in order to complete the real isobaric distribution. Using data from charge distribution total mass-yield distribution was obtained. The analysis of the mass-yield distribution allows to suppose existence of different channels of the interaction such as spallation, deep spallation, fission-like and multifragmentation processes.

PACS numbers: 25.45.-z, 25.60.Pj, 25.85.-w

## 1 Introduction

In recent years the attention of nuclear physicists has been directed towards understanding the mechanism of nucleus-nucleus interactions at energies of a few GeV per nucleon. The dependence of the formation cross section of a nuclide upon the bombarding energy of the projectile (the excitation function) has a characteristic shape which often can be related to the reaction mechanism. One of the questions concerning the reaction mechanism is how the projectile is interacting with target, partially or wholly. Comparisons of cross sections of different residuals are useful in pointing the similarities and differences between their reaction mechanisms. Investigation of deuteron-nucleus collisions is important since deuteron represents itself as the lightest weakly bounded system, hence during interaction with nucleus the characteristics of the interactions of the distinct nucleons can be derived.

In our recent works the deuteron induced reactions on separated tin isotopes were investigated [1]. The results obtained were compared with proton induced reactions, which allowed to make conclusions about the deuteron interaction mechanism. These results represent a great interest for the improvement of theoretical models. The experimental results can also be useful for astrophysics over space and accelerator technology and nuclear waste transmutation based on the accelerator-driven subcritical nuclear power reactors.

The gold is a frequently experimentally studied target among medium mass nuclei, which allows to track the evolution of the main characteristics of the different reaction channels adducting to formation of light residuals up to heavy ones. A considerable amount of measurements was performed for proton-induced reactions on gold target using various experimental methods [2–7]. The main goal of such studies was the extraction of the properties of different channels interaction by the analysis of large amount of experimental cross sections as well as the investigation of charge and mass distribution of the reaction products in wide range of energy up to 300 GeV.

An extensive abundance of data now exists from the study of intermediate and high energy heavy-ions on gold target [7–9]. Both the counter techniques and induced activity methods have been successfully employed in these studies. The calculation of the cross sections of formation of independent products and their integration over all fragment mass range allowed to estimate the total reaction cross section and to compare it to the data reported in literature. This comparison allows to specify the role of the projectile in the mechanism of nuclear reaction.

Gold target is attractive because different interaction channels are present in the experimental data and are available for comparison. On the other hand the mono-isotope composition of the Au element essentially facilitates the analysis of measurement data.

Nevertheless, a survey on the literature displays that there is a considerable lack of experimental data for the deuteron interaction with the gold target. They are mainly devoted to the study of the distinct reaction channels. There is a work about fission, induced at energy 2.1 GeV, where the cross sections for binary and ternary fission were measured using plastic detectors [10]. In the work of C. Damdinsuren *et al.* [11], at the interaction of 3.65 A GeV deuterons with Au, the cross sections of formation of spallation products were measured by direct counting of irradiated targets on Ge(Li) spectrometers. The set of the data was restricted by a little amount of products, which did not allow to make the complete analysis of the interaction. Until now, only one study of target residues formed during the fission reactions of deuterons with an energy of 4 GeV and gold was reported [12]. Measurements were made in the solid state nuclear track detector technique. Here, only the total fission cross section has been estimated and a suggestion has been made that the total fission cross section of  $^{197}\text{Au}$  is the same within the accuracy of measurements as for the fission, induced by protons with the same total energy.

The goal of the present experiment is to provide a set of experimental cross sections of formation of residuals in the reactions of deuterons with Au. The experimental data obtained will allow to estimate the contribution of different reaction channels such as fragmentation, spallation and fission-like processes, and to make a comparison with the earlier studies of the proton-induced reaction.

Here we should say that in high energy nuclear reaction products can be produced by spallation, deep spallation, fission, and multifragmentation processes. According to the J. Hufner [13] defined these processes in the following way:

1. spallation is the process in which only one heavy fragment with mass close to the target mass  $A_T$  is formed (a special case of spallation is the so-called deep spallation where  $M = 1$  but  $A \sim \frac{2}{3}A_T$ );
2. fission is the process in which  $M = 2$  and  $A$  is around  $A_T/2$ ;
3. multifragmentation is the process where  $M > 2$  and  $A < 50$ .

## 2 Experimental Procedure

A beam of 4.4 GeV deuteron from the Nuclotron of the VBLHEP, JINR was used to irradiate gold target. The target was the stack of gold foils with the size  $2 \times 2 \text{ cm}^2$ . Altogether 15 foils were used with the thickness of each target foil  $39.13 \text{ mg/cm}^2$ . The irradiation time was 28.6 hours at ion beam total intensity of about  $(6.43 \pm 0.71) \cdot 10^{12}$  deuterons. The reaction  $^{27}\text{Al}(d, 3p2n)^{24}\text{Na}$  with cross section of  $15.25 \pm 1.5 \text{ mb}$  [14] for beam monitoring was used. The  $\gamma$ -rays from the decay of residual nuclei formed in the target were measured, in an off-line analysis, with High purity Germanium (HpGe) detector with 28% relative efficiency and an energy resolution of 2 keV ( $^{60}\text{Co}$  at 1332 keV). The energy-dependent efficiency of the HpGe detectors was measured with standard calibration sources of  $^{54}\text{Mn}$ ,  $^{57,60}\text{Co}$ ,  $^{137}\text{Cs}$ ,  $^{154}\text{Eu}$ ,  $^{152}\text{Eu}$ , and  $^{133}\text{Ba}$ . The  $\gamma$  spectra were evaluated with the code package DEIMOS32 [15]. The residual radioactive nuclei were identified by the energy and intensity of characteristic  $\gamma$ -lines and by the respective half-lives of nucleus. Nuclear properties, used for identification of observed isotopes, were taken from literature [16]. The half-lives of identified isotopes were within the range of 15 min and 1 yr. The error in determining cross sections depended on the following factors: the statistical significance of experimental results ( $\leq 2\text{-}3\%$ ), the accuracy in measuring the target thickness and the accuracy of tabular data on nuclear constants ( $\leq 3\%$ ), and the errors in determining the detector efficiency with allowance for the accuracy in calculating its energy dependence ( $\leq 10\%$ ).

The fragment production cross sections are usually considered as an independent yield (I) in the absence of a parent isotope (which may give a contribution in measured cross section via  $\beta^\pm$ -decays) and are determined by using the following equation:

$$\sigma = \frac{\Delta N \lambda}{N_d N_n k \epsilon \eta (1 - \exp(-\lambda t_1)) \exp(-\lambda t_2) (1 - \exp(-\lambda t_3))} \quad (1)$$

where  $\sigma$  is the cross section of the reaction fragment production (mb);  $\Delta N$  is the area under the photopeak;  $N_d$  is the deuteron beam intensity ( $\text{min}^{-1}$ );  $N_n$  is the number of target nuclei (in  $1/\text{cm}^2$  units);  $t_1$  is the irradiation time;  $t_2$  is the time of exposure between the end of the irradiation and the beginning of the measurement;  $t_3$  is the measurement time;  $\lambda$  is the decay constant ( $\text{min}^{-1}$ );  $\eta$  is the intensity of  $\gamma$ -transitions;  $k$  is the total coefficient of  $\gamma$ -ray absorption in target and detector materials, and  $\epsilon$  is the  $\gamma$ -ray detection efficiency.

In the case where the cross section of a given isotope includes a contribution from the  $\beta^\pm$ -decay of neighboring unstable isobars, the cross section calculation becomes more complicated [17]. If the formation cross section of the parent isotope is known from experimental data, or if it can be estimated on the basis of other sources, the independent cross sections of daughter nuclei can be calculated by the relation:

$$\sigma_B = \frac{\lambda_B}{(1 - \exp(-\lambda_B t_1)) \exp(-\lambda_B t_2) (1 - \exp(-\lambda_B t_3))} \times \left[ \frac{(\Delta N)_{AB}}{N_d N_n k \epsilon \eta} - \sigma_A f_{AB} \frac{\lambda_A \lambda_B}{\lambda_B - \lambda_A} \left( \frac{(1 - \exp(-\lambda_A t_1)) \exp(-\lambda_A t_2) (1 - \exp(-\lambda_A t_3))}{\lambda_A^2} - \frac{(1 - \exp(-\lambda_B t_1)) \exp(-\lambda_B t_2) (1 - \exp(-\lambda_B t_3))}{\lambda_B^2} \right) \right], \quad (2)$$

where the subscripts  $A$  and  $B$  label variables referring to, respectively, the parent and the daughter nucleus; the coefficient  $f_{AB}$  specifies the fraction of  $A$  nuclei decaying to a  $B$  nucleus ( $f_{AB} = 1$ , when the contribution from the  $\beta$ -decay corresponds 100%); and  $(\Delta N)_{AB}$  is the total photopeak area associated with the decays of the daughter and parent isotopes. The effect of the precursor can be negligible in some limiting cases: where the half-life of the parent nucleus is very long, or in the case where its contribution is very small. In the case when parent and daughter isotopes can not be separated experimentally, the calculated cross sections are classified as cumulative ones (C). It should be mentioned that the use of induced-activity method imposes several restrictions on the registration of the reaction products. For example, it is impossible to measure a stable and very short-lived, very long-lived isotopes.

### 3 Results and Discussion

The experimental cross sections of reaction fragment production in the mass range of  $22 \leq A \leq 198$  amu are presented in Table I. Here, the types of cross sections (I-independent and C-cumulative) and the type of decay ( $\beta^-$  and EC) are also shown. As we can see from Table I most of residuals are the nuclei with  $\beta^+$  decay. It may be due to the fact that the average multiplicity of neutrons emitted from nucleus is a few times higher than the average multiplicity of protons in nuclear reactions [18].

In order to obtain a complete picture of the charge and mass distributions of the reaction products, it is necessary to estimate the cross sections of isotopes unmeasurable by the induced-activity method. For this purpose the charge distribution curve (i. e., the variation of cross section with  $Z$  value at constant  $A$ ) constructed on the base of independent cross section of the reaction products can be used. In the present work the analysis of the charge distributions was obtained using the expression from [3]:

$$\sigma(Z, A) = \sigma(A) \exp\left(-R|Z - SA + TA^2|^{3/2}\right), \quad (3)$$

where  $\sigma(Z, A)$  is the independent cross section for a given nuclide with atomic charge  $Z$  and a mass number  $A$ ;  $\sigma(A)$  is the total isobaric cross section of the mass  $A$ , and the parameters  $R$ ,  $S$  and  $T$  were fitted to the data from the spallation mass region to  $A = 40$  amu. Parameter  $R$  defines the width of the charge distribution and parameters  $S$  and  $T$  define the most probable charge ( $Z_p$ ) for a given isobar chain  $A$ .

In order to uniquely specify the variables  $R$ ,  $S$  and  $T$ , it will be necessary to measure more than four independent yield cross sections for each isobar. In case of shortage of the experimental data on the independent cross section another assumption was used for the construction of the charge distributions. This assumption is based on the similarity of the charge distribution curves for neighboring isobaric chains observed previously in different works [19, 20]. Thus cross sections of radionuclide from a limited mass range can be used to determine a single charge distribution curve. Taking into account the parent isotope cross section from the calculated isobaric-yield distribution using Eq. 2 the measured cross sections were adjusted on the precursor feeding where necessary.

During fitting procedure it was found that the values of  $R$  and  $S$  were unchanged for all mass range of the reaction products, but the parameter  $T$  was larger for the spallation fragments. This means that the width of the charge distribution at a given mass number is the same for all range of product mass number, but the most probable charge is smaller for lighter mass chains (i. e.,  $(Z - Z_p)$  difference is more neutron excessive). The values of these parameters for the 4.4-GeV deuterons are

$$R = 30A^{-0.79}, \quad S = 0.47, \quad T = 2.3 \times 10^{-4} \quad (4)$$

Using these values and the expression (3) the total isobaric cross section ( $\sigma_A$ ) was calculated for every mass number in the mass range  $40 \leq A \leq 130$  amu. The same values of  $R$  and  $S$  were used for the spallation mass range ( $A > 130$ )

but with parameter  $T = 3.2 \times 10^{-4}$ , which reflects the shift in the most probable charge to a smaller value than others mass ranges. The summing of all isobaric yields gives the total mass yield for the interaction channels in the given mass range of the residual nuclei. It should be mentioned that in frames of intranuclear cascade model the intermediate nuclear state with higher excitation energies results in a large number of the evaporated nucleons. Hence, a set of neutron-deficient nuclei are formed as a result of spallation, deep spallation and fission-like processes, which we have observed [21, 22]. The large number of the neutron evaporation is connected to the high excitation energy of after cascaded nucleus. Displacement of the charge distribution curves for residuals with  $A < 130$  to the neutron deficit side can be a result of contribution of the higher excited after cascaded nuclear states.

Fig. 1(a, b, c) shows the calculated partial cross sections (the ratio of cross section of fragment production to the total cross section with given mass number), as well as their Gaussian charge distribution, for different isobaric chains as a function of the difference  $(Z_p - Z)$ . An interesting feature is that the width of charge distribution of the present work is the same as for the system  $^{197}\text{Au}+p$  at the proton energy 1.0-3.0 GeV, but in this work the center of charge distribution for the mass  $A \leq 130$  amu shifted towards the neutron-deficient side of the valley of beta-stability. There is also a good agreement with the parameters  $S = 0.477$  and  $T = 2.4 \times 10^{-4}$  for the system  $^2\text{H}+^{181}\text{Ta}$  at the energy of deuterons 7.3 GeV [23]. It can be reposed that the charge distributions of the fragments are mainly determined by the properties of residual nuclei and don't depend on the way of their formation.

The isobaric yields obtained in this manner are shown as the filled squares in Fig. 2. The smooth curve on the Fig. 2 indicates the best fit for the mass number  $24 \leq A \leq 198$  amu based on the experimental data with the inclusion of contribution from different processes such as spallation, deep spallation or fission-like binary decay, and fragmentation or multifragmentation. The analysis of the cross sections distribution, depending on the product mass number or a number of the emitted nucleons, allows to make a definite assumption about mechanism of their formation. It can distinguish the regions of the specific channels of the fragments formation.

The residuals like  $^{196}\text{Au}$  and  $^{198}\text{Au}$  can be formed in the processes stripping or transition of one neutron. At the energies investigated in present work (2.2.Gev/nucleon) the nuclear interaction proceeds via surface collision with small energy transition. The experimentally determined cross section for deuterons with nuclei can be about 1.7 times more with respect to the proton-induced reaction. It can be seen from Table I that the probability of the neutron evaporation several times more than neutron transfer or other processes bring to the increasing mass number of the target nucleus. The cross section of neutron production in deuteron-nucleus reaction in the energy range of about GeV is larger than in proton-nucleus reaction because of stripping reaction [18]. The inelastic cross section of neutron-nuclear reactions in energy range several GeV is about  $1 - 2$  b [24]. Therefore the reaction  $(n, 2n)$  from the stripping neutrons can give the contribution in  $^{197}\text{Au}(d, X)^{196}\text{Au}$  reaction and can increase the cross section of our experimental data.

The region  $A > 131$  amu is connected to the spallation process with a characteristic decrease of the cross sections of the product formation on the number of the emitted nucleons.

The mass range  $60 \leq A \leq 120$  amu includes different channels of interaction indistinguishable in activation measurements. In our previous work it was marked, that in this region the approximately constant value of the excitation energy is preserved. It can be proposed that all the above mentioned processes (deep spallation, fission, fragmentation) contribute to the formation of residuals. In this range the energy transfer to the after cascaded remnants promotes the new reaction channel opening.

The intermediate mass fragments (IMFs) ( $40 < A < 60$ ) represent the group of fragments for which one can not say unequivocally that they are formed during the fragmentation mechanism. One of the possible ways of the origin of IMFs is that they represent the products in pair with  $A \sim 120 - 130$  amu. Or, for instance, deep spallation may be accompanied not only by emission of nucleons and light charge particles (with  $Z \leq 2$ ) but emission of IMFs is not excluded either. An alternative explanation of the origin of the products with  $A = 40 - 60$  amu was suggested by the intranuclear cascade model [25], according to which these fragments are the result of the disintegration of highly excited residual nucleus with  $A \sim 185$ .

In region of masses less than 40 amu can be a factor of phase transition at interaction that is connected with increasing excitation and transition to other kind processes as multifragmentation [26].

Integration of the mass-yield curves over mass number gives the cross section for the production of target residues  $2.20 \pm 0.44$  b. We have chosen a lower limit of 40 mass units because the multiplicity of fragments with masses smaller than  $\sim 40$  is unknown. These products may arise from interaction where another heavy fragment also survives and had thus already been counted.

Table I. The cross sections of nuclides formed by the reaction of 4.4 GeV deuterons with  $^{197}\text{Au}$ . Independent cross sections are indicated by (I); others are cumulative (C).

Element	Reac.(decay)	$\sigma, mb$	Element	Reac.(decay)	$\sigma, mb$
$^{24}\text{Na}$	C ( $\beta^-$ )	$8.02\pm 0.80$	$^{117m}\text{Sn}$	C ( <i>IT</i> )	$0.23\pm 0.02$
$^{28}\text{Mg}$	C ( $\beta^-$ )	$2.30\pm 0.66$	$^{124}\text{Sb}$	I ( $\beta^-$ )	$2.80\pm 0.60$
$^{42}\text{K}$	C ( $\beta^-$ )	$3.34\pm 0.13$	$^{126}\text{Sb}$	C ( $\beta^-$ )	$2.40\pm 0.46$
$^{43}\text{K}$	C ( $\beta^-$ )	$4.98\pm 1.70$	$^{119}\text{Te}$	C ( <i>EC</i> )	$0.66\pm 0.09$
$^{47}\text{Ca}$	C ( $\beta^-$ )	$0.70\pm 0.16$	$^{132}\text{Te}$	C ( $\beta^-$ )	$2.93\pm 0.88$
$^{44}\text{Sc}$	I ( <i>EC</i> )	$1.76\pm 0.70$	$^{124}\text{I}$	I ( <i>EC</i> )	$0.46\pm 0.03$
$^{44m}\text{Sc}$	I ( <i>EC</i> )	$0.45\pm 0.16$	$^{126}\text{I}$	I ( <i>EC</i> , $\beta^-$ )	$2.02\pm 0.34$
$^{46}\text{Sc}$	I ( $\beta^-$ )	$4.05\pm 0.46$	$^{133}\text{I}$	C ( $\beta^-$ )	$1.22\pm 0.16$
$^{48}\text{Sc}$	I ( $\beta^-$ )	$1.71\pm 0.71$	$^{127}\text{Xe}$	C ( <i>EC</i> )	$10.92\pm 1.20$
$^{48}\text{V}$	C ( <i>EC</i> )	$1.14\pm 0.09$	$^{131}\text{Ba}$	C ( <i>EC</i> )	$14.94\pm 1.23$
$^{52}\text{Mn}$	C ( <i>EC</i> )	$0.66\pm 0.09$	$^{140}\text{Ba}$	C ( $\beta^-$ )	$0.79\pm 0.08$
$^{54}\text{Mn}$	I ( <i>EC</i> )	$3.59\pm 0.69$	$^{139}\text{Ce}$	C ( <i>EC</i> )	$11.71\pm 0.95$
$^{59}\text{Fe}$	C ( $\beta^-$ )	$1.81\pm 0.36$	$^{143}\text{Ce}$	C ( $\beta^-$ )	$7.37\pm 1.60$
$^{55}\text{Co}$	C ( <i>EC</i> )	$2.26\pm 0.72$	$^{143}\text{Pm}$	C ( $\beta^-$ )	$12.94\pm 0.96$
$^{56}\text{Co}$	C ( <i>EC</i> )	$0.34\pm 0.10$	$^{144}\text{Pm}$	C ( <i>EC</i> )	$1.54\pm 0.14$
$^{58}\text{Co}$	I ( <i>EC</i> )	$3.77\pm 0.15$	$^{148m}\text{Pm}$	I ( $\beta^-$ )	$1.10\pm 0.29$
$^{60}\text{Co}$	C ( $\beta^-$ )	$3.22\pm 0.47$	$^{145}\text{Eu}$	C ( <i>EC</i> )	$14.36\pm 2.00$
$^{65}\text{Zn}$	C ( <i>EC</i> )	$4.29\pm 0.33$	$^{146}\text{Eu}$	I ( <i>EC</i> )	$18.12\pm 1.80$
$^{72}\text{Zn}$	C ( $\beta^-$ )	$0.16\pm 0.09$	$^{147}\text{Eu}$	I ( <i>EC</i> )	$34.00\pm 3.00$
$^{71}\text{As}$	C ( <i>EC</i> )	$0.30\pm 0.04$	$^{148}\text{Eu}$	I ( <i>EC</i> )	$1.09\pm 0.17$
$^{72}\text{As}$	C ( <i>EC</i> )	$3.40\pm 0.22$	$^{149}\text{Eu}$	C ( <i>EC</i> )	$19.16\pm 1.42$
$^{74}\text{As}$	I ( <i>EC</i> )	$3.02\pm 0.24$	$^{146}\text{Gd}$	C ( <i>EC</i> )	$13.24\pm 2.08$
$^{75}\text{Se}$	C ( <i>EC</i> )	$4.82\pm 0.12$	$^{147}\text{Gd}$	I ( <i>EC</i> )	$6.23\pm 1.20$
$^{77}\text{Br}$	C ( <i>EC</i> )	$2.18\pm 0.42$	$^{149}\text{Gd}$	I ( <i>EC</i> )	$17.86\pm 0.58$
$^{82}\text{Br}$	I ( $\beta^-$ )	$1.68\pm 0.05$	$^{153}\text{Gd}$	I ( <i>EC</i> )	$9.70\pm 0.90$
$^{81}\text{Rb}$	C ( <i>EC</i> )	$5.92\pm 0.66$	$^{147}\text{Tb}$	C ( <i>EC</i> )	$2.99\pm 0.50$
$^{83}\text{Rb}$	I ( <i>EC</i> )	$7.17\pm 0.90$	$^{149}\text{Tb}$	C ( <i>EC</i> )	$5.39\pm 0.97$
$^{84}\text{Rb}$	I ( <i>EC</i> )	$3.20\pm 0.30$	$^{153}\text{Tb}$	C ( <i>EC</i> )	$4.01\pm 0.97$
$^{83}\text{Sr}$	C ( <i>EC</i> )	$4.04\pm 0.07$	$^{160}\text{Tb}$	I ( $\beta^-$ )	$8.94\pm 0.80$
$^{85}\text{Sr}$	C ( <i>EC</i> )	$10.30\pm 2.10$	$^{167}\text{Tm}$	C ( <i>EC</i> )	$21.80\pm 3.20$
$^{86}\text{Y}$	C ( <i>EC</i> )	$6.21\pm 0.88$	$^{168}\text{Tm}$	I ( <i>EC</i> , $\beta^-$ )	$2.62\pm 0.18$
$^{87}\text{Y}$	C ( <i>EC</i> )	$8.93\pm 1.02$	$^{171}\text{Lu}$	C ( <i>EC</i> )	$26.75\pm 3.00$
$^{88}\text{Y}$	C ( <i>EC</i> )	$6.01\pm 0.80$	$^{172}\text{Lu}$	C ( <i>EC</i> )	$4.16\pm 0.42$
$^{88}\text{Zr}$	C ( <i>EC</i> )	$9.44\pm 0.50$	$^{173}\text{Lu}$	C ( <i>EC</i> )	$25.16\pm 1.80$
$^{89}\text{Zr}$	C ( <i>EC</i> )	$7.26\pm 0.90$	$^{177m}\text{Lu}$	C ( $\beta^-$ )	$1.36\pm 0.30$
$^{95}\text{Zr}$	C ( $\beta^-$ )	$0.7\pm 0.38$	$^{175}\text{Hf}$	C ( <i>EC</i> )	$27.14\pm 3.00$
$^{90}\text{Nb}$	C ( <i>EC</i> )	$4.80\pm 0.94$	$^{181}\text{Hf}$	C ( $\beta^-$ )	$2.41\pm 0.24$
$^{92m}\text{Nb}$	I ( <i>EC</i> , $\beta^-$ )	$0.38\pm 0.04$	$^{182}\text{Ta}$	C ( $\beta^-$ )	$2.75\pm 0.75$
$^{95}\text{Nb}$	I ( $\beta^-$ )	$1.09\pm 0.30$	$^{182}\text{Re}$	C ( <i>EC</i> )	$48.97\pm 9.40$
$^{95m}\text{Nb}$	C ( $\beta^-$ )	$0.35\pm 0.03$	$^{184g}\text{Re}$	I ( <i>EC</i> )	$0.92\pm 0.18$
$^{93}\text{Tc}$	C ( <i>EC</i> )	$3.46\pm 0.42$	$^{184m}\text{Re}$	I ( <i>EC</i> )	$4.09\pm 0.25$
$^{94}\text{Tc}$	C ( <i>EC</i> )	$2.67\pm 0.34$	$^{185}\text{Os}$	I ( <i>EC</i> )	$28.95\pm 5.40$
$^{96}\text{Tc}$	I ( <i>EC</i> )	$2.25\pm 0.30$	$^{185}\text{Ir}$	C ( <i>EC</i> )	$26.88\pm 2.18$

Continue of the Table 1.

$^{103}\text{Ru}$	C ( $\beta^-$ )	$1.32\pm 0.13$	$^{190}\text{Ir}$	I ( $EC$ )	$4.09\pm 0.80$
$^{99}\text{Rh}$	C ( $EC$ )	$4.92\pm 0.07$	$^{192}\text{Ir}$	I ( $EC, \beta^-$ )	$3.12\pm 0.70$
$^{100}\text{Rh}$	I ( $EC$ )	$2.13\pm 0.12$	$^{194m}\text{Ir}$	C ( $\beta^-$ )	$1.13\pm 0.10$
$^{102}\text{Rh}$	I ( $EC, \beta^-$ )	$3.85\pm 0.60$	$^{188}\text{Pt}$	C ( $EC$ )	$27.35\pm 8.00$
$^{102m}\text{Rh}$	I ( $EC, \beta^-$ )	$13.15\pm 1.50$	$^{191}\text{Pt}$	C ( $EC$ )	$14.95\pm 3.50$
$^{100}\text{Pd}$	C ( $EC$ )	$1.31\pm 0.36$	$^{194}\text{Au}$	C ( $EC$ )	$26.61\pm 2.00$
$^{105}\text{Ag}$	C ( $EC$ )	$8.06\pm 1.10$	$^{195}\text{Au}$	C ( $EC$ )	$15.41\pm 2.60$
$^{106m}\text{Ag}$	I ( $EC, \beta^-$ )	$2.31\pm 0.40$	$^{196}\text{Au}$	I ( $EC, \beta^-$ )	$140.82\pm 12.82$
$^{110m}\text{Ag}$	I ( $EC, \beta^-$ )	$0.32\pm 0.02$	$^{198g}\text{Au}$	I ( $\beta^-$ )	$1.56\pm 0.25$
$^{111}\text{In}$	C ( $EC$ )	$8.03\pm 1.10$	$^{198m}\text{Au}$	I ( $\beta^-$ )	$7.41\pm 0.50$
$^{113}\text{Sn}$	C ( $EC$ )	$17.43\pm 1.98$			

For comparison we have calculated the total reaction cross section using the hard sphere model [27] for nucleus-nuclear interactions. This model refers to the overlap of the two sharp spheres forms of interacting nuclei and the total reaction cross section is presented in terms of a two-parameters expression:

$$\sigma_R = \pi r_0^2 (A_T^{1/3} + A_p^{1/3} - b_{Tp})^2 fm^2, \quad (5)$$

where  $A_T$  and  $A_p$  are the mass numbers of the target and projectile nuclei, respectively;  $r_0$ , is the constant of proportionality in the expression of geometrical nuclear radius  $r_i = r_0 A_i^{1/3}$  and  $b_{Tp}$  is the overlap parameter. The quantity  $b_{Tp}$  is equal to  $\Delta r / r_0$  where  $\Delta r$  is the geometrical overlap between the colliding nuclei.

Because the total reaction cross section is known from our experimental data, the impact parameter  $b$  can be estimated using the above mentioned expression. From estimated overlap parameter  $b_{Tp} = 0.97$  fm in the present experiment the mean value of the impact parameter  $b$  equals to 8.37 fm was obtained.

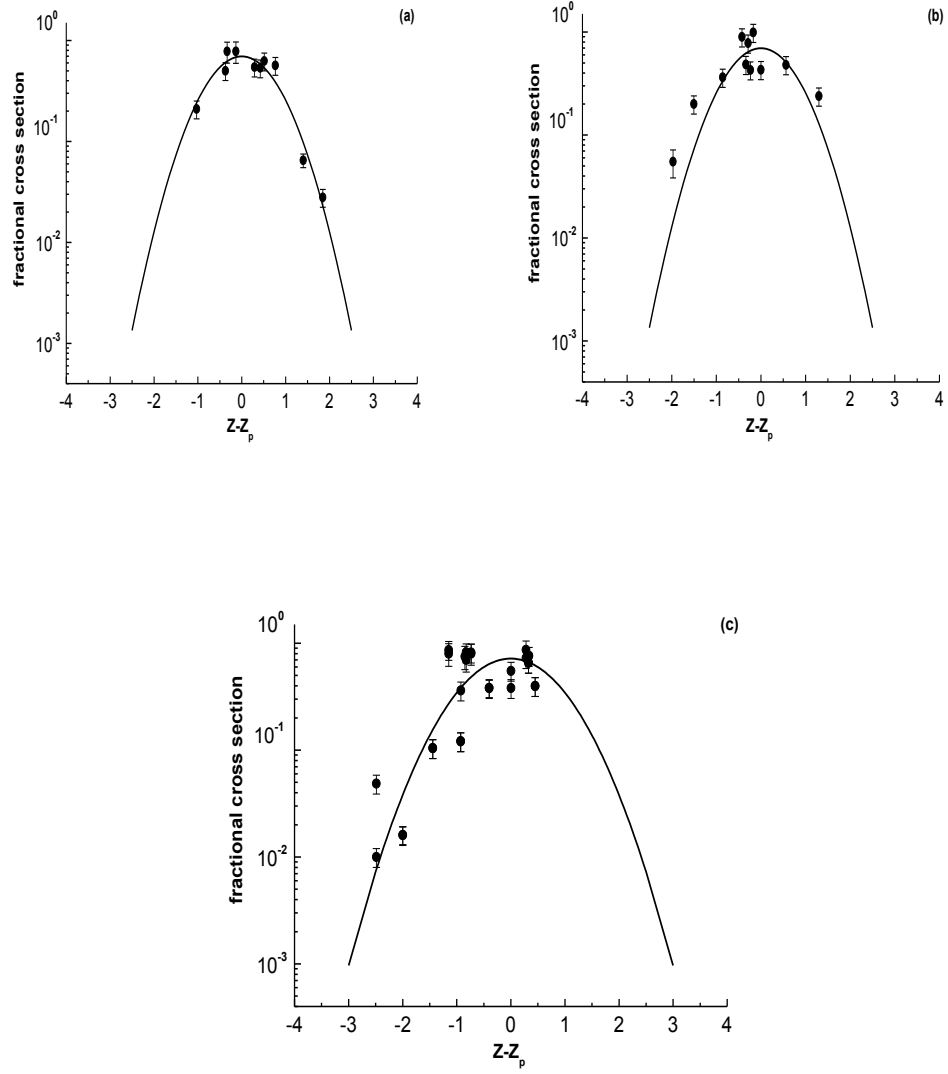


FIG. 1: The charge distributions of the soobaric chains in the mass regions: (a)=42-65; (b)=83-127; (c)=133-198 for the 4.4 GeV deuteron-induced reaction on  $^{197}\text{Au}$ ; ●-experimental data; solid line is fit by expression (3) .

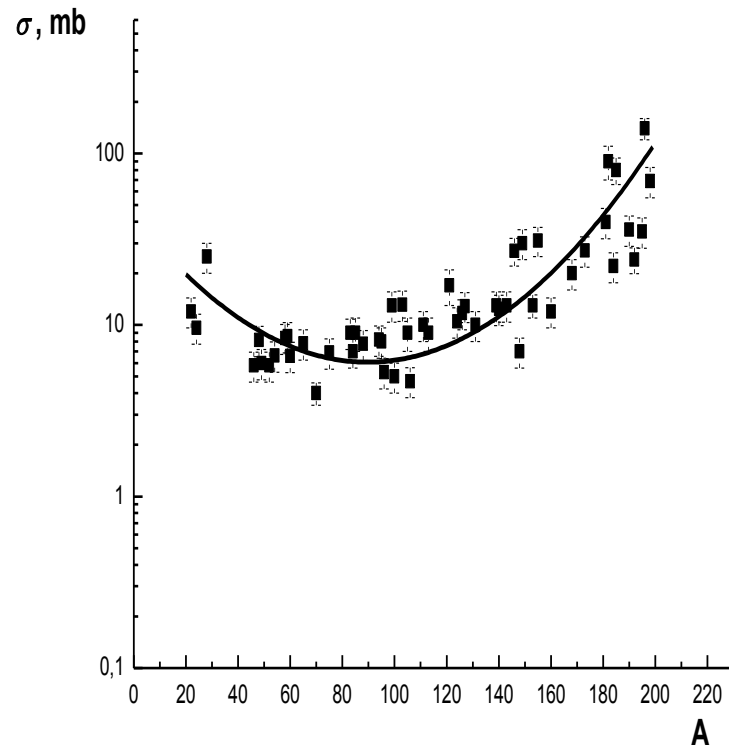


FIG. 2: Mass-yield distribution of 4.4 GeV deuteron-induced reaction on  $^{197}\text{Au}$ . Solid squares indicate estimated total isobaric cross sections, solid line is the best fit through the experimental cross sections of the reactions fragments.

Since the value of impact parameter lies in the range  $1/2(R_p + R_T) \leq b \leq (R_p + R_T)$  [9], we can conclude that the collision on the whole is peripheral. It can be suggested that in peripheral collisions at large impact parameter the probability of the interaction of deuteron as whole is very low. Taking into account the low coupling energy in



deuteron (2.22 MeV) it can be presented that in this case only one nucleon of deuteron interacts with the target. This assumption has been confirmed by the theoretical work [18]. The value of  $b$  of the present work is larger than value  $b = 7.45$  for the system  ${}^2\text{H}+{}^{197}\text{Au}$  at the energy 7.3 GeV [11] and can indicate a more peripheral interaction at higher incident energy.

One of the main questions concerning the reaction mechanism is the energy transfer in relativistic nucleus-nucleus collisions. In this regard, it is interesting to compare our experimental data with the similar results of the reactions of high energy protons and deuterons. In Figs. 3 and 4 the ratios of cross section of residuals from the reactions of 4.4 GeV deuterons on the gold target of the present work and of 3.65 GeV/nucleon [23] and 3.0 GeV [3] protons with  ${}^{197}\text{Au}$ , respectively, were shown. The results can be presented in frames of the two basic concepts of high-energy nuclear physics, such as factorization and limiting fragmentation [28]. The first hypothesis assumes that the yield of particular fragment from the target decay during the nuclear interactions will not be dependent on the beam except the geometric factor.

Thus, fragmentation cross sections for the reaction  $P + T \rightarrow F + X$ , where  $P$  and  $T$  are the projectile and target, and  $F$  is the fragment, produced during the reaction, can be factored according to  $\sigma_{T,P}^F = \sigma_T^F \gamma_p$ , where  $\gamma_p$  is dependent only on the projectile. Hence, for the reactions with protons and deuterons the ratio of cross sections is

$$\sigma^F(d + {}^{197}\text{Au})/\sigma^F(p + {}^{197}\text{Au}) = \gamma_d/\gamma_p, \quad (6)$$

which should have constant values  $\gamma_d/\gamma_p$  for any residuals. It means that the ratio should be equal to the ratio of the total cross sections of reactions.

The ratio of experimental cross sections was determined for target residues in the mass region from  $A = 24 - 196$ . The average values of the relative projectile factors of our work and data from [23] and [3] were  $\gamma_d/\gamma_p = 1.2 \pm 0.2$  and  $1.55 \pm 0.24$ , respectively. The ratio of total reaction cross sections of the present work and data for [23] is equal  $1.37 \pm 0.34$ . So it can be supposed that in the investigated energy range the hypothesis of factorization has been accomplished.

The hypothesis of limiting fragmentation states that the distribution of products in the rest frame of the projectile or target approaches a limiting form as the bombarding energy increases or, experimentally, that a particular distribution changes negligibly over a large range of bombarding energies. In order to test this hypothesis, we compared our results with the deuteron data on the gold target at 7.3 GeV [11]. The ratios of cross section of residuals are shown in Fig. 5. The average values of the relative projectile factor in this case were equal  $1.63 \pm 0.24$  and total cross section ratio was  $0.7 \pm 0.1$ . From the obtained results we can conclude that the limiting fragmentation is not valid for high energy deuterons interactions.

For comparison with model representation of the spallation reactions induced by protons and deuteron in Au nucleus the intra-nuclear cascade and following evaporation for description of the spallation process were considered in [18]. Using the parametrization obtained in [18] the mean multiplicity of emitted particles (neutrons and protons, other charged particles compose a small part) for deuteron- proton- and neutron-induced reactions on gold target at the same energy were calculated. The values of these multiplicities are  $\langle n \rangle = 31.121(10\%)$  for  $d+{}^{197}\text{Au}$  reaction,  $\langle n \rangle = 21.03(10\%)$  for  $p+{}^{197}\text{Au}$  and  $\langle n \rangle = 21.33(10\%)$  for  $n+{}^{197}\text{Au}$  reaction at the energy 2.2 GeV/nucleon. As we can see, the total neutron multiplicity in deuteron-induced reactions is less than the sum of the total neutron multiplicity in proton-induced reactions and of the same quantity in neutron-induced reactions, for the same target and the same incident energy per nucleon. The non-additivity of the cascades initiated by the neutron and the proton contained in the deuteron comes from two facts. First, for peripheral collisions, one of the nucleons may not interact at all, corresponding to a stripping reaction. Second, for more central collisions, the propagation of one of the nucleons "clears the space" seen by the other nucleon.

The ratio of multiplicities of emitted particles in deuteron- and proton-nuclear reactions is  $1.5 \pm 0.2$  should correspond to the cross section ratio of the residual nuclei formation in average. This value is in a satisfactory agreement with our experimental results.

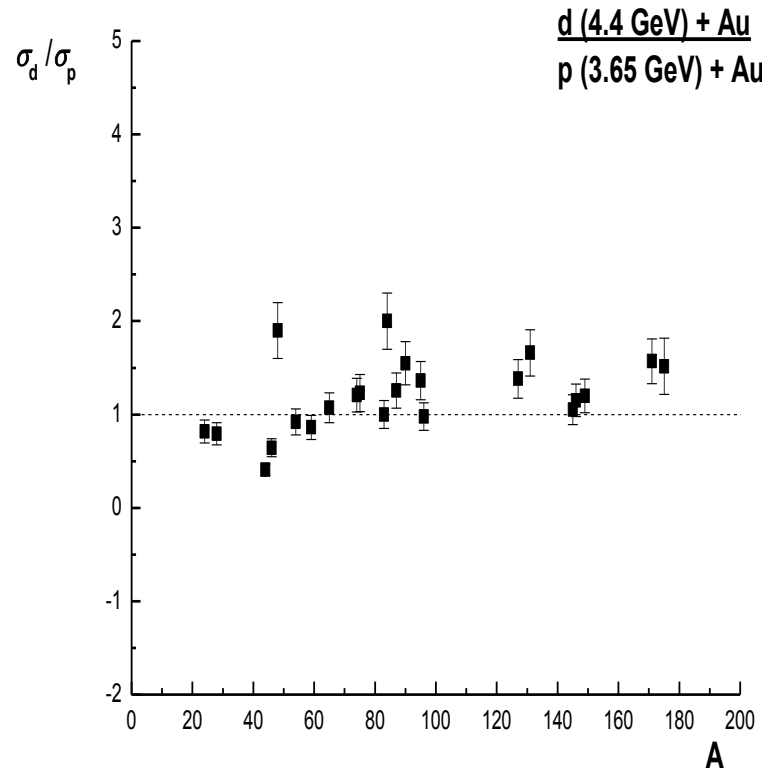


FIG. 3: The ratio of experimental cross sections  $\sigma_d/\sigma_p$  of residuals from the reactions of 4.4 GeV deuterons with gold of present work and 3.65 GeV protons with  $^{197}\text{Au}$  [23].

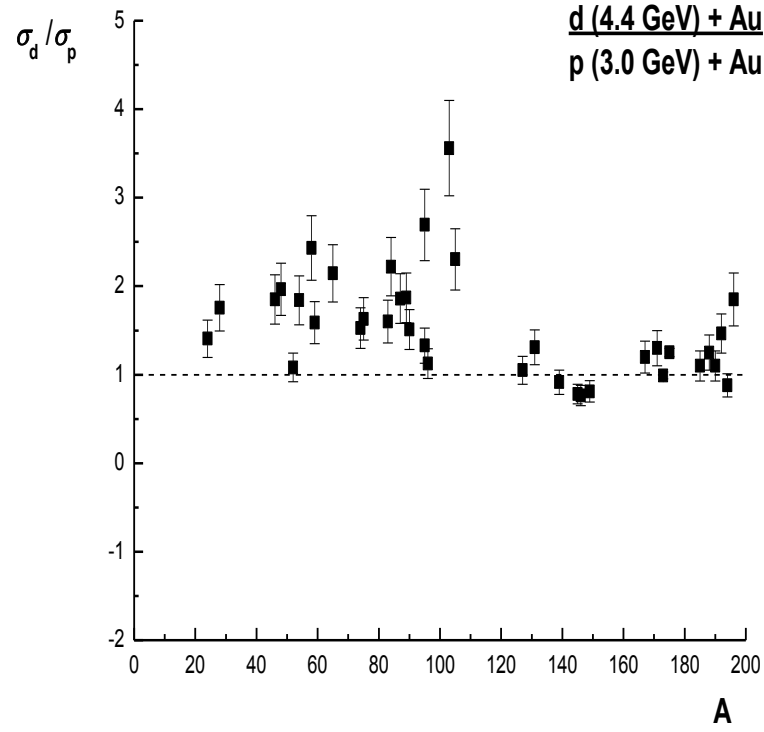


FIG. 4: The ratio of experimental cross sections  $\sigma_d/\sigma_p$  of residuals from the reactions of 4.4 GeV deuterons with gold of present work and 3.0 GeV protons with  $^{197}\text{Au}$  [3].

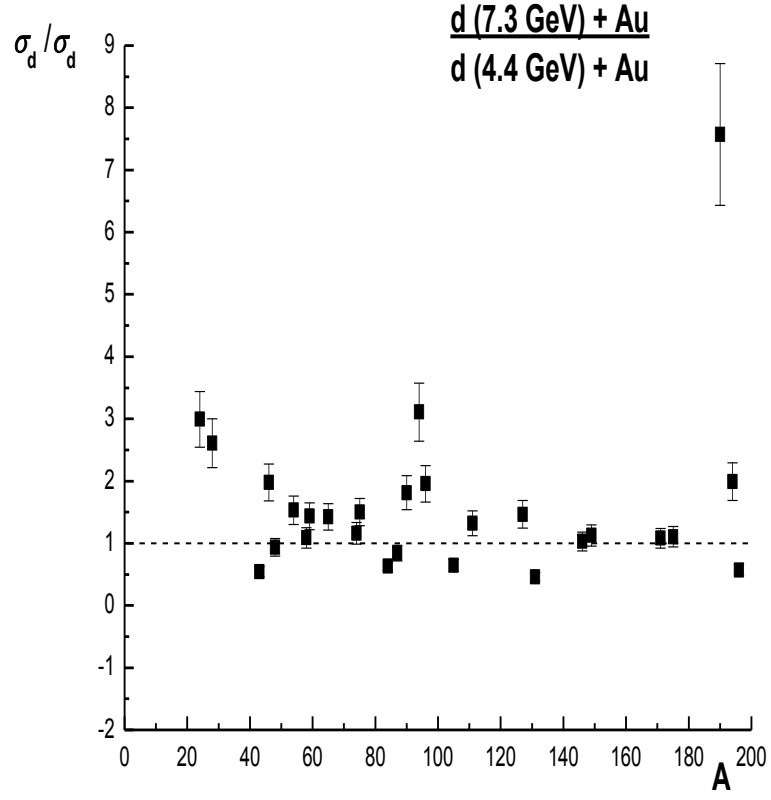


FIG. 5: The ratio of experimental cross sections  $\sigma_d/\sigma_d$  of residuals from the reactions of 7.3 GeV deuterons [11] with gold target and the data of present work of 4.4 GeV deuterons with  $^{197}\text{Au}$ .

#### 4 Conclusion

The cross sections of more than 100 radioactive products formed in the reaction of deuterons with  $^{197}\text{Au}$  have been measured at bombarding energy of 4.4 GeV. The charge distribution was analyzed in the term of 3-parameter equation. It was found that the width of the charge distribution at a given mass number is the same for all range of product mass number, but the most probable charge is smaller for the lighter mass chains. The mass yield distribution of target residues has been determined by integration of the cross sections for fragments with  $A > 40$  and has been compared with the theoretical predictions. It was suggested that a few sources having different excitation energies can take part in the formation of residual nuclei, fission, production of the IMFs and spallation.

The calculation of the impact parameter indicates that target residues from the reactions of 4.4 GeV deuterons with gold are created in peripheral collisions.

The ratio of the experimental cross sections of proton and deuteron induced reactions is in a good agreement with the ratio of theoretical calculations of the multiplicity of the emitted particles in the cascade and evaporation stages.

The mechanism of interaction of deuteron with nucleus is not provided by the additional interaction of two nucleons in deuteron in the interaction with nuclei. The deuteron as weak bound nucleus can decay and demonstrate one nucleon collision in most cases of interactions. The interaction was of peripheral character in most cases as it was estimated from the calculation of the impact parameter of deuteron-nucleus interaction.

The similarity between the cross section of target residues of this work and those from the reactions with proton- and deuteron-induced reactions on the gold target at the different kinetic energies may be viewed as an evidence for factorization in these reactions. The condition of the limiting fragmentation is not valid for the energy deuterons up to 7.3 GeV.

The ratio of the cross sections of proton- and deuteron-induced reactions can confirm the fulfilling of the factorization conditions in the investigated energy range.

#### Acknowledgment

G. Karapetyan is grateful to Fundação de Amparo à Pesquisa do Estado de São Paulo (FAPESP) 2011/00314-0 and to International Centre for Theoretical Physics (ICTP) under the Associate Grant Scheme.

The authors are grateful to group leader of LNP JINR Dr. S. Avdeev for granting possibility of carrying out experiment, and also to lead researcher of LHEP JINR Kh. Abraamyan for the help during the experiment.

- 
- [1] A. R. Balabekyan, A. S. Danagulyan, J. R. Drnoyan *et al.*, *Physics of Atomic Nuclei* **69**, 1485 (2006).
  - [2] R. Michel, R. Bodemann, H. Busemann *et al.*, *Nucl. Instrum. Methods B* **129**, 153 (1997).
  - [3] S. B. Kaufman and E. P. Steinberg, *Phys. Rev. C* **22**, 167 (1980).
  - [4] S. B. Kaufman, M. W. Weisfield, E. P. Steinberg *et al.*, *Phys. Rev. C* **14**, 1121 (1976).
  - [5] A. Letourneau, A. Bohma, J. Galina *et al.*, *Nucl. Phys. A* **712**, 133 (2002).
  - [6] S. R. Hashemi-Nezhad, I. Zhuk, A. Potapenko *et al.*, *Nucl. Instrum. Methods A* **679**, 82 (2012).
  - [7] P. Kozma and C. Dandinsuren, *Czech. J. Phys. B* **40**, 38 (1990).
  - [8] J. Gindler, H. Monzel, J. Buschmann *et al.*, *Nucl. Phys. A* **145**, 337 (1970).
  - [9] D. J. Morrissey, W. Loveland, M. de Saint Simon, and G. T. Seaborg, *Phys. Rev. C* **21**, 1783 (1980).
  - [10] F. Rahimi, D. Gheysari, G. Remy *et al.*, *Phys. Rev. C* **8**, 1500 (1973).
  - [11] C. Dandinsuren, V. Iljushchenko, P. Kozma *et al.*, *Yad. Fiz.* **52**, 330 (1990).
  - [12] S. Stoulos, W. Westmeier, R. Hashemi-Nezhad *et al.*, *Phys. Rev. C* **85**, 024612 (2012).
  - [13] J. Hufner, *Phys. Rep.* **125**, 129 (1985).
  - [14] J. Banaigs *et al.*, *Nucl. Instrum. Methods A* **95**, 307 (1971).
  - [15] J. Frána, *J. Radioanal. Nucl. Chem.* **257**, 583 (2003).
  - [16] R. B. Firestone, in *Tables of Isotopes*, 8th ed.: 1998 Update (with CD ROM), edited by S. Y. Frank Chu (CD-ROM editor) and C. M. Baglin (Wiley Interscience, New York, 1996).
  - [17] H. Baba, J. Sanada, H. Araki *et al.*, *Nucl. Instrum. Methods A* **416**, 301 (1998).
  - [18] J. Cugnon, C. Volant, S. Vuillier, *Nucl. Phys. A* **625**, 729 (1997).
  - [19] H. Kudo, M. Maruyama, and M. Tanikawa *et al.*, *Phys. Rev. C* **57**, 178(1998).
  - [20] C. L. Branquihno and V. J. Robinson, *J. Inorg. Nucl. Chem.* **39**, 921 (1977).
  - [21] V. M. Maslov, *Nucl. Phys. A* **717**, 3 (2003).
  - [22] M. C. Duijvestijn, A.J. Koning *et al.*, *Phys. Rev. C* **59**, 776 (1999).
  - [23] P. Kozma, J. Kliman, M. Leonard, *Czech. J. Phys. B* **38**, 973 (1988).

- [24] V. S. Barashenkov and V. D. Toneev, Interactions of High-Energy Particles and Nuclei with Nuclei (Atomizdat, Moscow,1972)
- [25] Y. Yariv and Z. Fraenkel, Phys. Rev. C **20**, 2227 (1979).
- [26] R. Wolfgang, E. W. Baker, A. A. Karetto *et al.*, Phys. Rev. **103**, 394 (1956).
- [27] H. L. Bradt and B. Peters, Phys. Rev. **77**, 54 (1950).
- [28] R. P. Feynman, Phys. Rev. Lett. **23**, 1415 (1969).
- [29] J. Benecke, T. T. Chou, C. N. Yang, and E. Yen, Phys. Rev. **188**, 2159 (1969).